JACS
JOURNAL OF THE AMERICAN CHEMICAL SOCIETY
Article
pubs.acs.org/JACS

Valence Bond Theory Reveals Hidden Delocalized Diradical Character of Polyenes

Junjing Gu,[†] Wei Wu,*[,†] David Danovich,[‡] Roald Hoffmann,*[,§] Yuta Tsuji,[∥] and Sason Shaik*[,‡]

[†]The State Key Laboratory of Physical Chemistry of Solid Surfaces, *i*ChEM, Fujian Provincial Key Laboratory of Theoretical and Computational Chemistry and College of Chemistry and Chemical Engineering, Xiamen University, Xiamen, Fujian 361005, China

[‡]Department of Organic Chemistry and the Lise Meitner-Minerva Centre for Computational Quantum Chemistry, The Hebrew University, Jerusalem 91904, Israel

[§]Baker Laboratory, Department of Chemistry and Chemical Biology, Cornell University, Ithaca, New York 14853, United States

[∥]Education Center for Global Leaders in Molecular Systems for Devices, Kyushu University, Nishi-ku, Fukuoka 819-0395, Japan

Supporting Information

ABSTRACT: The nature of the electronic-structure of polyenes, their delocalization features, and potential diradicaloid characters constitute a fundamental problem in chemistry. To address this problem, we used valence bond self-consistent field (VBSCF) calculations and modeling of polyenes, $C_{2n}H_{2n+2}$ (n = 2−10). The theoretical treatment shows that starting with n = 5, the polyene's wave function is mainly a shifting 1,4-diradicaloid, a character that increases as the chain length increases, while the contribution of the fundamental Lewis structure with alternating double and single bonds (**1**) decays quite fast and becomes minor relative to the diradicaloid pack. We show how, nevertheless, it is this wave function that predicts that polyenes will still exhibit alternating short/long CC bonds like the fundamental structure **1**. Furthermore, despite the decay of the VB contribution of **1**, it remains the single structure with the largest weight among all the individual structures. The mixing of all the 1,4-diradicaloid structures into **1** follows perturbation theory rules, with the result that the delocalization energy due to this mixing is additive and behaves as a linear function of the number of the double bonds, $\Delta E_{del} = -6.9 \times n$ (kcal mol^{-1}). The VB modeling shows that while the conjugation stabilizes structure **1**, this stabilization energy is energetically overridden by the Pauli repulsion between two adjacent double bonds. Nevertheless, unsubstituted polyenes remain planar; this observation is addressed. Potential manifestations of the diradicaloid nature of polyenes are discussed, and it is concluded that the diradicaloid character is clearly not a well-defined physical property as in real diradicals. Thus, we went full circle to realize that our philosophical question may not be strictly resolved. The localized/delocalized properties of polyenes seem to define a "chemical duality principle". This duality of molecular wave functions is a ubiquitous beguiling phenomenon.

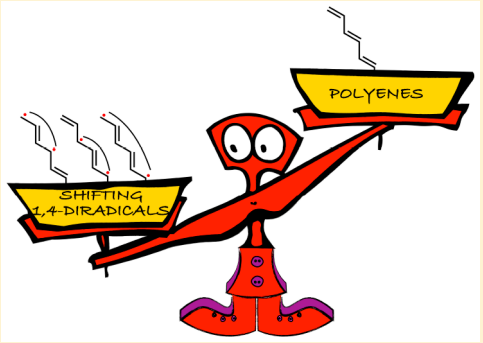

1. INTRODUCTION

Only slightly behind benzene and cyclobutadiene, linear polyenes $C_{2n}H_{2n+2}$ (in Scheme 1) have formed a traditional springboard for testing theoretical concepts and thereby served to sharpen insight into electronic structure. This fundamental significance,[1] together with their role in life-sustaining systems such as the mechanism of vision and light harvesting systems, and as conducting polymers, etc. have made polyenes very popular among chemists and physicists.[1a] Understanding the electronic structure of polyenes is therefore always a fundamental issue.

There is a peculiar dichotomy in the way we think of the electronic structure of polyenes. In some respects they behave as though they were electronically localized species, composed of double bonds separated by single bonds and representable by the classical structure **1** (Scheme 1). In contrast to this localized picture, polyenes exhibit collective electronic phenomena, which point to a highly delocalized π-electronic structure seemingly at odds with **1**. Let us elaborate a bit the two sides of this coin starting from the evidence for a localized presentation and moving on to the delocalized one.

Experimental and computational[1−3] data reveal that polyenes possess alternating short double bonds (1.36−1.38 Å) and long single bonds (1.44−1.47 Å). As such, the structural data provide support for a description such as **1**, where the double bonds are localized and maintain rather weak interactions that modify a bit the lengths of the double and single bonds. Incidentally, the experimental value of the single bond C−C distance of polyene is very close to the C−C bond length (1.44−1.45 Å), which was determined recently by theoretical means for the reference states of double bonds with nonbonded 2p(π) electrons.[4] Other evidence comes from the rotational behavior of polyenes which features small barriers (5.9 kcal

Received: May 4, 2017
Published: June 13, 2017

DOI: 10.1021/jacs.7b04410
J. Am. Chem. Soc. 2017, 139, 9302−9316

Scheme 1. Classical Representation of Polyenes (1) with Their Alternating Bond Length R_{CC} Values, the Dewar Resonance Energy Stabilization and $\pi-\pi$ Repulsion (2), and the Two VB Structures (3a, 3b) that Describe Butadiene in VB Theory

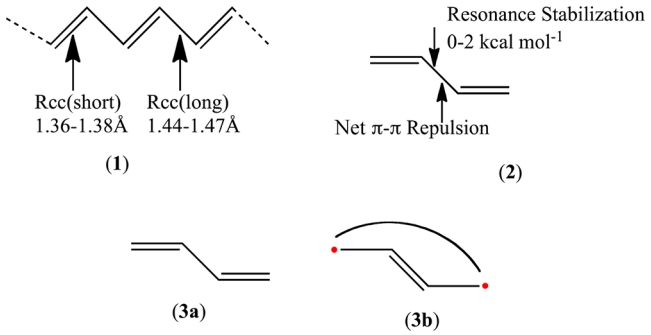

mol^{-1}) around the formal "single" C−C bonds and large ones (35−45 kcal mol^{-1}) corresponding to the "double" C═C bonds.

M. J. S. Dewar[5] showed early on that despite the common wisdom that polyenes are delocalized, their π-energy is additive such that the double bond−double bond interaction "is absorbed into the properties of the single bonds". As such, he argued, the single classical structure **1** provides a simple and convenient description, which from a practical point of view has advantages that outweigh any theoretical deficiencies. Subsequently,[5b] he showed that the resonance effects in polyenes are small and any stability of the polyene reflects the stronger sp^2-sp^2 σ-bonds. Using various semiempirical methods, Dewar estimated the $\pi-\pi$ resonance effect across the single bond to be 0−2 kcal mol^{-1}, as shown in **2** in Scheme 1, and noted[5a] that inclusion of overlap in his calculations reduces greatly the bond order of the central bond, thus implying that the $\pi-\pi$ Pauli repulsion may outweigh this small value of the π−resonance energy. The very small resonance interaction estimated by Dewar et al. was close to the experimentally estimated 2−3.4 kcal mol^{-1} using heats of hydrogenation by Kistiakowsky and Conant.[6]

Over the ensuing five decades, this polyenic $\pi-\pi$ resonance value across a single bond has been re-estimated by many workers using approaches such as isodesmic reactions and energy decomposition analyses (EDA) of various sorts. The values typically oscillated between the low end, 1−4 kcal mol^{-1},[7−9] and the somewhat higher end of 8−10 kcal mol^{-1}.[10,11] In an EDA study of conjugation, Frenking and coworkers[12] found a 19.5 kcal mol^{-1} attractive π orbital component to the total energy of interaction of butadiene. This conjugative interaction is balanced, however, by some fraction of the ca. 98 kcal mol^{-1} repulsive sum of the electrostatic and Pauli repulsion terms,[12] but it is impossible to partition these by orbital symmetry type, as one can with the orbital interaction contribution. The most recent value of the conjugation energy, 12.6 kcal mol^{-1}, was reported by Mo et al.[13] using the block-localized wave function (BLW) approach.[14] Mo also noted that the accepted experimental resonance energy (ERE) was 8.5 kcal/mol. It is important to note that Dewar[5b] used the small polyenic resonance energy (~2 kcal mol^{-1}) as a reference for his thermochemical resonance energy (TRE) scale for cyclic systems such as benzene. Due to the work of Schaad and Hess,[15] the TRE scale became a standard in organic chemistry, but this is based now on a higher value (~9 kcal mol^{-1})[16] of the polyenic resonance energy.

As we mentioned, Dewar[5a] already implied that the net interaction of two π bonds in a polyene may be repulsive. Others came to a similar conclusion based on overlap populations.[7] Recently, Nascimento et al.[17a,b] used a generalized product wave function, made of strongly orthogonal π-pairs to construct a "quasiclassical" state (QCS), and thereby partitioned the total energy into the energy of the QCS and the "interference energy" due to delocalization. In so doing, they showed that the "delocalization/interference energy" in butadiene[17a] and other conjugated polyenes[17b] is dominated by $\pi-\pi$ repulsion, while the QCS is responsible for the stability of the polyene, its short "single" C−C bonds separating the double bonds, as well as for the rotational barriers around these bonds.[17a] As shown by Nascimento et al, the π-bonds in the QCS like **1**, are stabilized by lowering their kinetic energy, which is the criterion for covalent bonding following the pioneering study of Ruedenberg.[17c] From a different angle, Mo et al. showed the coexistence of stabilizing conjugative interaction and Pauli repulsion between the two conjugated π bonds.[13] The Pauli repulsion and stabilizing interaction coexist also in benzene and other aromatic molecules.[16] These features of bond alternation and basically small conjugative interactions portray an effective behavior embodied in the classical structure **1** in Scheme 1.

In contrast, and in all other respects, polyenes exhibit what might be called collective or delocalized electronic phenomena (e.g., in their electronic spectra, photoelectron spectra, semiconductivity, isomerization via solitons etc.); all of which indicate highly delocalized π-electronic structure seemingly incompatible with **1** in Scheme 1. Thus, long polyenes are photoconductors with a finite small gap,[1a] indicating delocalized molecular orbitals (MOs) which make up valence and conduction bands which approach one another due to antibonding interactions between the local π orbitals, and bonding interactions among the antibonding π^* orbitals.[18] UV−vis electronic absorption spectroscopy of substituted polyenes has been modeled effectively by a maximally delocalized particle-in-a-box model.[19] And polyene spectra show effects of hyperconjugation.[1b,20] Perhaps the most compelling evidence comes from photoelectron spectroscopy (PES) that indicates that all the MOs from which the photoelectron is being ejected are delocalized, such that one can even trace the nodes leading to antibonding interactions in these orbitals based on the fine structure of the PES peaks.[21] Indeed, the canonical MOs, which arise from any MO calculations are delocalized and thereby strengthen the impression that polyenes are delocalized. As such, these features show that polyenes exhibit a highly delocalized electronic structure very remote from representation **1** and unrepresentable by a simple VB structure.

Part of the difficulty here arises from a kind of chemical "duality principle." It has been known for some time that one can move by a unitary transformation between localized and delocalized molecular orbitals.[22] Any observable that depends on all the occupied orbitals (e.g., total energy, total dipole moment, etc.) can be discussed and calculated equivalently in the localized or delocalized basis. For observables that depend on one or a subset of molecular orbitals (ionization potential, spectra, for instance) one can start out with either set as well, but if one begins with localized orbitals, one in the first approximation is led to degeneracies that force one to take

DOI: 10.1021/jacs.7b04410
J. Am. Chem. Soc. 2017, 139, 9302−9316

linear combinations that are precisely the delocalized or canonical orbitals.[23]

Despite the evidence that supports either one of the two representations, the localized representation **1** in Scheme 1 is still the one used by most chemists. It appears in all textbooks, and it serves chemists very well in thinking about structure and reactivity of polyenes. This creates what seems to be an undesirable situation for such a fundamental and classical problem of electronic structure. Cannot one answer a simple question: are polyenes localized or delocalized? The problem may be with the question, not with providing an answer. It is like asking whether light is a particle or a wave. We shall see this clearly at the end of the manuscript.

It is clear from the above discussion that the dichotomy should be addressed at the level of a properly correlated wave function. The chemist's representation of a polyene, **1** in Scheme 1, is a VB structure; one of the many canonical structures which can be written for a polyene.[3] VB theory is a multireference theory. As such, VB theory is deemed appropriate to address this fundamental question by use of canonical structures.

VB theory has been applied before to butadiene and higher polyenes, using different brands of the theory as well as projection of MO−CI wave functions to VB structures.[3,24−32] Thus, using a projection technique, Berry[24] has reported being struck by the large ionic contribution to the wave function of butadiene. He ascribed the short central C−C bond to polarization. In another context, major interest focused on the covalent excited states of polyenes; the hidden excited state 2^1A_g of butadiene[33] which becomes the first excited state starting from C_8H_{10}[3,25,33,34] and the $1^1B_u^-$ excited state.[29]

We shall use here the VB self-consistent field (VBSCF) method[35] which has proven to be useful and efficient for handling polyenes and similar molecules.[32] As a VB structure-set, we use the canonical VB structures (called the Rumer structures[36]), which will allow us to decide how important structure **1** is, what other structures become important as the polyene grows, why is the energy additive, and whether there is a stabilizing interaction between the double bonds.

This work will endeavor to answer the questions posed above and demonstrate something unexpected: the dominant part of the wave function of polyenes (starting from $C_{10}H_{12}$ or $C_{12}H_{14}$) actually involves a shifting 1,4-diradical of the type apparent already in butadiene, **3b** versus **3a** in Scheme 1. In this sense, our study will touch base with other findings of diradical and polyradical characters in conjugated systems, using a variety of computational and experimental techniques.[37] As we will demonstrate, the family of these diradical structures increases as the polyene grows, while the pristine localized structure (of the type **1**) gradually diminishes. Nevertheless, it will be seen that the energy behaves as though the polyene were a collection of weakly interacting double bonds, **1**. For completeness we shall show the origins of the 2^1A_g and $1^1B_u^-$ excited states, and their relations to the polyenic structure **1**, and its diradical siblings.

2. METHODS

Geometry optimization of C_4H_6−$C_{28}H_{22}$ was done using B3LYP/D95V as implemented in Gaussian 09.[38,39] We tried also BHLYP and tested the results against MP2. Thus, B3LYP gave results compatible with MP2, whereas BHLYP performed less well and the results are relegated to the Tables S1-1−S1-3. All the VB calculations were carried out at the VBSCF method[35] with the XMVB, which is an ab initio valence bond program.[40] The D95V basis set was used for most of the cases. In some cases where long bonds made convergence difficult (using the bond distorted orbitals; see later), we used also STO-6G.[41a] The delocalization energy for butadiene was tested with other basis sets including cc-pVTZ, which gave results virtually identical to D95V (see Table S4B).[41b]

3. VBSCF METHOD

The VBSCF method uses a wave function which is a linear combination of VB structures Φ_K with coefficient C_K as shown in eq 1,

$$\Psi = \sum_K C_K \Phi_K \tag{1}$$

where each VB structure is a multideterminantal wave function corresponding to a specific chemical structure, and each VB determinant is constructed from occupied atomic orbitals [here, the 2p(π) orbitals, the generators of the π system]. The coefficients C_K are determined by solving the secular equation in eq 2, in the usual variational procedure.

$$\mathbf{HC} = E\mathbf{MC} \tag{2}$$

Here **H**, **M**, and **C** are the Hamiltonian, Overlap, and Coefficient matrices, respectively, while E is the total energy of the system (including the σ frame). The variational procedure involves a double optimization on the coefficients C_K, as well as the atomic orbitals of the VB structure, in a given atomic basis set. The σ-frame is treated as a set of doubly occupied MOs (taken from the corresponding Hartree−Fock wave function) that are not optimized during the VBSCF procedure. Thus, the VBSCF method is analogous to CASSCF in the sense that both methods optimize structure coefficients as well as the orbitals within the used atomic basis set. We use here the double-ζ D95V and the STO-6G basis sets.[39,41a]

The VB structures Φ_K are the Rumer structures assembled from VB determinants. Rumer structures are the canonical structures, which for a polyene $C_{2n}H_{2n+2}$ constitute all the modes of pairing the $2n$ π-electrons into n pairs. For a general polyene $C_{2n}H_{2n+2}$ in a singlet spin state, there exist m Rumer structures in the structure-set given in eq 3:

$$m = \binom{2n}{n} - \binom{2n}{n-1} \tag{3}$$

Diagonalization of the Rumer basis set provides a spectrum of covalent states, the lowest of which is the ground state, which is the focus of the present paper. Other states of interest here are the 2^1A_g and $1^1B_u^-$ covalent excited states.[3]

3.1. Types of Atomic Orbitals in VBSCF. In describing the VB structures, one can use atomic orbitals (AOs), such that the Rumer structures will be purely covalent. We shall refer to this level of calculations as VBSCF(AO-C). Figure 1a shows a typical AO for butadiene. In addition to covalent structures, there are also many, many ionic structures, which can be added to the Rumer set, and this of course will increase very steeply the number of VB structures. For example, even for the small polyene C_8H_{10}, with 8-π electrons the full covalent-ionic structure-set contains a total of 1764 VB structures. And in a calculation by Hirao and Nakano[42] on butadiene, as in the Berry paper cited, one can see that the contribution of all the ionic structures is greater than that of the fundamental covalent one. In our AO-C basis calculations, we simply omit all the ionic structures and use only the covalent pairings.

DOI: 10.1021/jacs.7b04410
J. Am. Chem. Soc. 2017, 139, 9302−9316

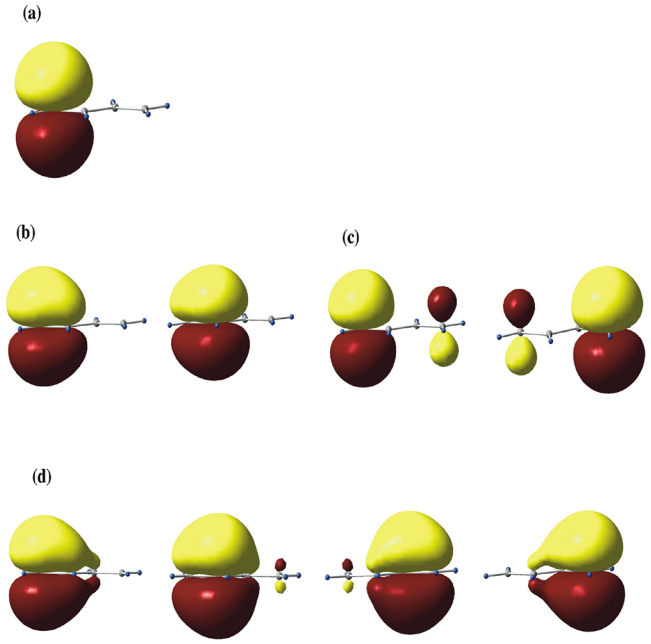

Figure 1. Atomic orbital types used in VBSCF: (a) pure AO for C_4H_6. (b) The two BDOs for the terminal C1−C2 bond of C_4H_6 (see structure **3a** in Scheme 1). (c) The two BDOs for the long C1−C4 bond (see structure **3b** in Scheme 1). Note the antibonding between the C1 and C4 contributions. (d) OEOs for C1, C2, C3, and C4 (in C1 and C4 the terminal tails are very small and virtually invisible here).

To avoid this multitude of ionic structures, there are ways to account for these structures effectively, while conserving the original number of Rumer structures. This is achieved by allowing the AOs to have small delocalization tails on atoms other than the one the AO "belongs" to. In this manner, ionic structures get embedded into the formally covalent Rumer structures (see pp. 40−42 in ref 23).[23] One such set of orbitals is called BDO,[43] where BDO stands for a bond distorted orbital in which each AO on a given atom is allowed to have a tail only on the atom to which it is bonded. As such, there are eight BDOs, which participate in all the possible bonding interactions in butadiene. The pair of BDOs describing the C1−C2 terminal π-bond of butadiene is shown in Figure 1b. One can see that each orbital is centered on one of the C atoms of the terminal bond but having a tail on the other atom; the tail is quite substantial, which indicates the importance of ionic structures in this π-bond. The same description will apply to the other terminal bond, C3−C4.

Interestingly, the BDOs for the long bond in Figure 1c also possess a substantial delocalization tail. However, the negative combination in BDO(1,4) shows that the corresponding ionic structures mixed in an antibonding fashion. This was verified by calculating the Coulson Bond Order[44] for the complete VBSCF calculations (see Scheme S3 and Tables S9 and S10). We further verified that the nature of this long bond BDO is sensitive to the number of electrons enclosed by the diradical; for 4-electrons in butadiene, BDO(1,4) is antibonding (where 1,4 indicate the numbers of the bonded carbon atoms), while BDO(1,6) in hexatriene is bonding, and again antibonding for BDO(1,8) in octatetraene (see Tables S9 and S10 and Scheme S3). This $4m/4m + 2$ dichotomy reflects that a cyclic delocalization is interrupted for 4m electrons but not for $4m + 2$ electrons. We shall refer to this method as VBSCF(BDO-C), where the C denotes that the number of Rumer structures is identical to the covalent set.

The second type of semilocalized AOs are those used commonly in the GVB and SC VB methods.[45,46] These orbitals have a long tradition in chemistry and are appropriately called "Coulson-Fisher" AOs after a seminal paper by C. A. Coulson and I. Fischer in which they were introduced.[47] These "AOs" are here called OEOs, where the term stands for overlap-enhanced orbitals. In OEOs, the AO has the freedom to have a tail on all other atoms in the molecule.[48] As such, butadiene has four unique OEOs, each being centered more on one of the atoms C1, C2, C3, or C4 while having smaller tails on all others. For the sake of a uniform terminology, we shall refer here to this level as VBSCF(OEO-C), where again the number of VB structures is identical to the covalent Rumer set. Figure 1d shows the four OEOs; one centered more on C1, the second on C2, and two OEOs on C3 and C4 related to C2 and C1 by symmetry. One can see that now each OEO has contribution from four carbons. Thus, in both BDOs and OEOs, the tails are apparent. They bring into a calculation based formally only on covalent functions the ionicity that would occur in an AO-based VB computation. It is perhaps noticeable that while the BDO pair is intuitively clear, the OEO pairs are less so when the semidelocalization is quite extensive.

The VBSCF(BDO-C) and VBSCF(OEO-C) methods are more accurate than the VBSCF(AO-C). Nevertheless, for all the properties calculated here, the trends in VBSCF(AO-C) were found to be virtually identical to those from VBSCF-(BDO-C) or VBSCF(OEO-C).

In the VB calculations, one of course includes covalent structures where the electrons are singlet paired over long distances, such 1−4 in a polyene, or more distant pairings. We will call these "long bonds." These long bonds are common to VBSCF(AO-C), VBSCF(BDO-C), and VBSCF(OEO-C). In the latter AO types, the long bond primarily (albeit not exclusively) exists between the atoms having the largest contribution to the two spin coupled AOs.

3.2. Rumer Structure-Set for Polyenes. Figure 2 shows the hierarchy of the Rumer structure-set for a generic polyene with n π-electron pairs. The total number of the structures is given by eq 3. These structures spread into blocks of constant numbers of long-bonds and relative energy, which ascends as the number of long bonds increases. The energy parameter is given by λ, which is the energy cost of breaking a short bond (see Section 1), as explained before.[3] The first block has a single Rumer structure, which is the fundamental classical structure that possess n-short π-bonds (like **1** in Scheme 1), and is labeled as $R(0)$, here the parenthetical zero indicates that all the bonds are intact and there are no long bonds, namely, no diradicaloids.

Above $\boldsymbol{R}(0)$, there is a block, $\boldsymbol{R}(1)$, which is composed of a set of Rumer structures, labeled as $R(1,j)$, where j is an index that indicates the number of short π-bonds that are broken in the given structure. The "red" electrons that appear in the valence structure are singlet paired; we will call such valence structures diradicaloid (or long bond structures). Thus, the index j is the number of short π-bonds separating the "radical" centers. As such, the subset $R(1,1)$ involves those VB structures in which paired long bonds are separated by a single short π-bond, thus forming what we will call a 1,4-diradicaloid, as depicted in Figure 2 for one member of the $R(1,1)$ set. We depict the long bond of the diradicaloid as a curved line that connects the singlet-paired electrons. What is being implied is

DOI: 10.1021/jacs.7b04410
J. Am. Chem. Soc. 2017, 139, 9302−9316

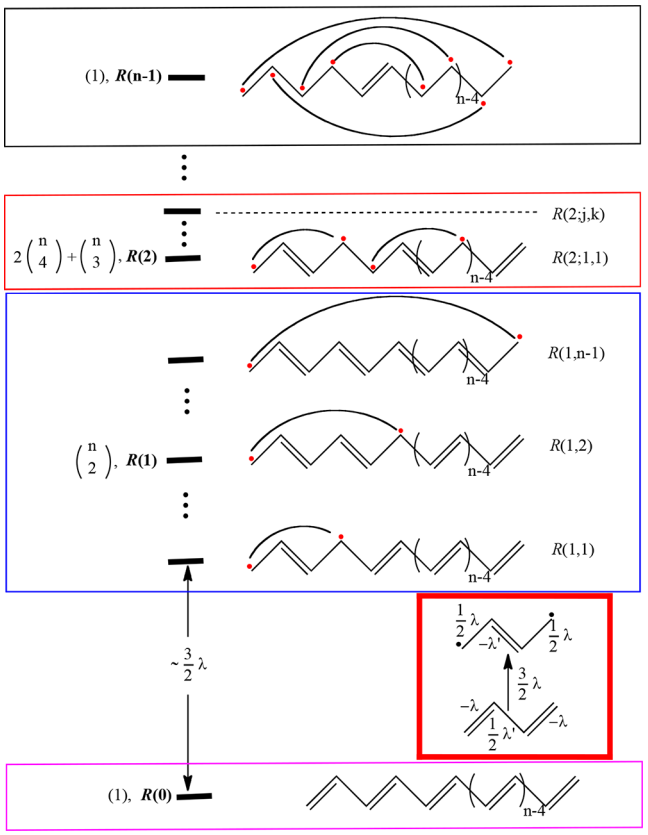

Figure 2. Spectrum of the Rumer structure-set for n-electron pairs over $2n$ centers. The inset shows the energy cost (in units of λ; see Section 1) involved in creating a diradicaloid by breaking two short π bonds and creating one π bond across the original single C−C bond and long bond between the diradical centers. The red-framed inset shows the elementary excitation involved in creating a long bond from two short ones. The elementary excitation is given as $(3/2)\lambda$, assuming for simplicity that $\lambda = \lambda'$. Blocks are indicated by bold $\boldsymbol{R}$, while individual structures are indicated by regular font symbols [e.g., R(i,j)].

nothing more or less than a singlet pairing in a covalent wave function.

In $\boldsymbol{R}(1)$, there is also a group of $R(1,2)$ structures in which the radicals are separated by two short π bonds, a situation that creates what we call a 1,6-diradicaloid. One $R(1,2)$ structure is depicted in Figure 2. This continues all the way to $R(1,n-1)$ where the electrons in the $(1,n-1)$-diradicaloid are placed at the termini of the polyene and are separated by $n-1$ π bonds. All the $R(1,j)$ structures are obtained from the $R(0)$ structure by breaking original short π bonds while pairing the electrons across the original single C−C bonds which are the longer bonds. As such, the structure $R(1,n-1)$ is of the highest energy in the $\boldsymbol{R}(1)$ block. And in general, the number of intervening bonds between the diradicaloid pair determines the energy ordering in this subset. The number of Rumer structures in block $\boldsymbol{R}(1)$ is

$$d_1 = \binom{n}{2} \tag{4}$$

The energy ordering of the blocks is determined by the number of short bonds broken to make diradicaloid species. Thus, above $\boldsymbol{R}(1)$ there lies the block of $\boldsymbol{R}(2)$ structures, which involve two diradicaloid species. The number of Rumer structures in block $\boldsymbol{R}(2)$ is

$$d_2 = 2\binom{n}{4} + \binom{n}{3} \tag{5}$$

One of them is depicted as an example. It is labeled as $R(2;1,1)$ which signifies two diradicaloid pairs, each being separated by a π bond. This continues up to the $\boldsymbol{R}(n-1)$ block which possess a single Rumer structure having $n-1$ diradicaloid species, as shown at the top of Figure 2. For a general case, a Rumer structure with m diradicaloids can be labeled as $R(m; l_1,l_2,...,l_m)$, where l_i stands for the number of carbon pairs by which the i-diradicaloid is separated. The carbon pair may be either a short π bond or a diradicaloid.

The energy spacing between the Rumer blocks is determined by the number of short π-bonds that are broken relative to the fundamental structure $\boldsymbol{R}(0)$. The inset, between the $\boldsymbol{R}(0)$ and $\boldsymbol{R}(1)$, in Figure 2 shows the elementary excitation in converting two short π-bonds to a 1,4-diradicaloid and a π-bond across the original single C−C bond. Each short π-bond is stabilized by $-\lambda$.[3] However, the π-bonds repel one another by the Pauli repulsion between the identical electrons. Thus, each electron in a π-bond or in a diradicaloid is 50% α and 50% β, and hence, the Pauli repulsion between the π bond and the diradicaloid is twice the term $+0.5\lambda$ (consult Section 1). If we ignore the fact that there is bond alternation and assume all λ values to be identical then the excited structure with the 1,4-diradicaloid and a π-bond lies above the elementary structure by $3/2(\lambda)$. Given that the strength (λ) of a π-bond[3] is of the order of 50 kcal mol^{-1} (at r_{av} = 1.4 Å), the energy gap involved in the elementary excitation in Figure 2 is on the order of 75 kcal mol^{-1}.

The energy difference between Rumer structures that belong to a single block is hard to express in a simple equation but very simple to comprehend qualitatively based on the inset in Figure 2. One can see that in the elementary excitation, we are converting a short π bond having a bonding interaction strength of $-\lambda$ to a longer π bond, across the original C−C single bond, with a bonding interaction strength of $-\lambda'$ where $|\lambda| > |\lambda'|$. At the same time, we create stronger Pauli repulsive interactions $2 \times (0.5\lambda)$ across the two short distances, due to the diradicaloid flanking the new π bond. Therefore, the more π bonds intervene between the diradicaloid in a given block, the higher the energy of the respective Rumer structure. For this reason, $R(1,n-1)$ is of the highest energy in the $\boldsymbol{R}(1)$ block, and so on.

Using C_6H_8, as an example, Scheme 2 arranges the respective five Rumer structures in blocks. As usual, $\boldsymbol{R}(0)$ is a block by itself, while $\boldsymbol{R}(1)$ contain three Rumer structures: two $R(1,1)$ types and one $R(1,2)$ type. And finally, $\boldsymbol{R}(2)$ contains a single Rumer structure with two long bonds.

Scheme 2. Rumer Blocks and Structures for C_6H_8

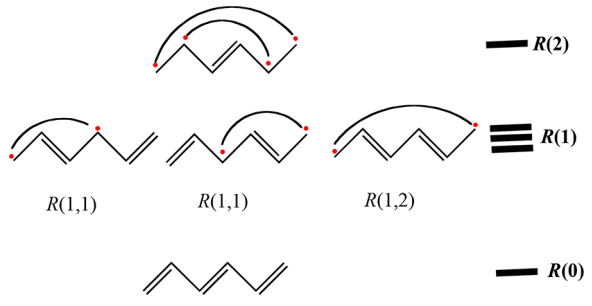

DOI: 10.1021/jacs.7b04410
J. Am. Chem. Soc. 2017, 139, 9302−9316

Scheme 3. (a) VB Mixing Diagram between Rumer Structures Φ_i and Φ_j, Using Perturbation Theory, (b) Schematic Representation of the Variation of the Reduced Matrix Element between the Fundamental Rumer Structure, $R(0)$, and Structures Belonging to the $R(1,j)$ Block, (c) Schematic Representation of the Variation of the Reduced Matrix Element between the Fundamental Rumer, $R(0)$, and Rumer Structures Belonging to a Single Block, $R(k; k > 1)$, Where k Changes from 1 and up[a]

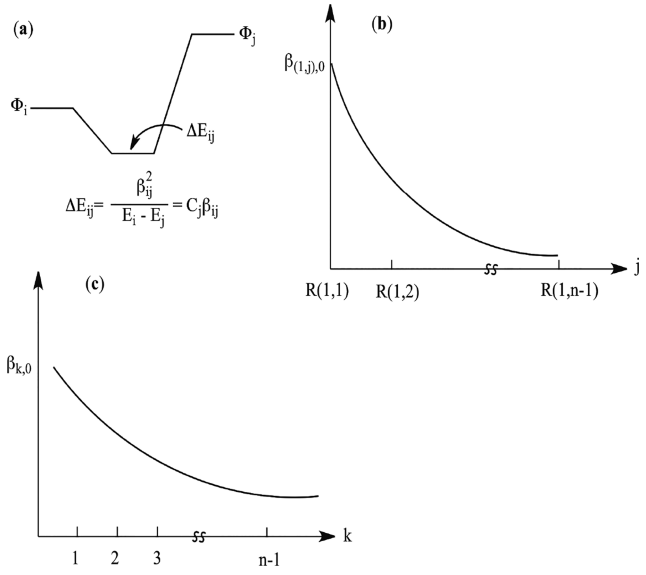

[a]Note that in both (b) and (c), the reduced matrix element falls off with j and k.

3.3. Interaction Rules for Mixing Rumer Structures for Polyenes. The rules for mixing matrix elements were derived in the previous work.[3] Basically, the mixing follows rules of perturbation theory, which is shown in Scheme 3a that describes the mixing of Rumer structures Φ_j into a lower lying Φ_i. Thus, following perturbation theory, this mixing depends on the energy gap between the structures, $(E_i - E_j)$, and their reduced matrix element, β_{ij} (see pp 45−69 in ref 23).[23] For overlapping wave functions as the Rumer structures, the requisite matrix element is the reduced matrix element[3,49] β_{ij} between Rumer structures Φ_i and Φ_j, given by

$$\beta_{ij} = H_{ij} - E_i S_{ij} \tag{6}$$

where H_{ij} is the corresponding Hamiltonian matrix element, S_{ij} the overlap, and E_i is the self-energy of the lower-lying Rumer structure Φ_i. Since the energy due to the mixing is $\beta_{ij}^2/(E_i - E_j)$, while the mixing coefficient of Φ_j into Φ_i is given by $C_j = \beta_{ij}/(E_i - E_j)$, then the energy contribution due to the mixing can be estimated from the computational output using the very simple equation:

$$\Delta E_{ij} = C_j \beta_{ij} \tag{7}$$

All the terms in eq 7 are easily available from the calculation, so one can determine the resonance energy contributions of all the excited Rumer structures by their mixing with the fundamental structure, $R(0)$.

3.3.1. Patterns and Trends of Reduced Matrix Elements in Polyenes. The dependence of the reduced matrix elements on the nature of the Rumer structures involved was derived in previous work (see Section 1, a−c).[3] Consider the reduced matrix elements between the fundamental Rumer structure, $R(0)$, and an excited structure belonging to the block $\boldsymbol{R}(k)$. On the basis of generalized Slater rules, it is clear that the more electron-shifts are involved in generating $\boldsymbol{R}(k)$ from $\boldsymbol{R}(0)$, the smaller is their reduced matrix element β_{0k}. This is basically the same behavior as the corresponding overlap S_{k0}, which falls off with the number of bond shifts (sh)[3] as follows: $S_{k0} = (-1/2)^{sh}$. The decay of this overlap is fast, and it affects the corresponding reduced matrix element. For example, Scheme 3b shows the trend by focusing on the reduced matrix elements between $R(0)$ and Rumer structures $R(1,j)$ belonging to block $\boldsymbol{R}(1)$. Thus, the larger the distance between the diradical centers in a given $R(1,j)$, the more electron shifts are required to generate it from $R(0)$ and the smaller is the corresponding $\beta_{(1,j),0}$. The largest matrix element will be found for $R(0)$ with the members of the $R(1,1)$ subset and the smallest for the $R(0)$ and the $R(1,n-1)$ structure (see Section 1, a and c).

Similarly, as shown in Scheme 3c, the reduced matrix elements $\beta_{k,0}$ between $R(0)$ and the $\boldsymbol{R}(k)$ Rumers from a block k, decrease the higher in energy the block is. Once again this has to do with the fact that the wave functions become different when the more electron shifting takes place to create $R(k)$ from $R(0)$.

These considerations are applied later in the discussion section.

4. RESULTS

4.1. Geometries and VB Wave Functions of Polyenes. Table 1 collects the B3LYP/D95V optimized bond lengths of $C_{2n}H_{2n+2}$ polyenes for n = 2−10. The well-known picture of bond alternation is apparent, and it seems to match reasonably well the fundamental structure, $R(0)$, of these polyenes. Note, however, that the terminal "double" bonds are shorter than internal double bonds, and the lengths of these double bonds

Table 1. C−C Bond Lengths[a] (in Å) of $C_{2n}H_{2n+2}$ Polyenes[b]

n	r_1	r_2	r_3	r_4	r_5	r_6	r_7	r_8	r_9	r_{10}
2	1.355	1.467								
3	1.358	1.459	1.365							
4	1.359	1.457	1.368	1.450						
5	1.359	1.456	1.370	1.447	1.372					
6	1.359	1.456	1.370	1.446	1.374	1.444				
7	1.360	1.456	1.371	1.445	1.375	1.442	1.376			
8	1.360	1.455	1.371	1.445	1.375	1.442	1.377	1.441		
9	1.360	1.455	1.371	1.445	1.375	1.441	1.377	1.440	1.377	
10	1.360	1.455	1.371	1.444	1.376	1.441	1.377	1.439	1.378	1.439

[a]B3LYP/D95V optimized values (unit in Å). [b]r_i means the unique bond length of C_i and C_{i+1}

DOI: 10.1021/jacs.7b04410
J. Am. Chem. Soc. 2017, 139, 9302−9316

Table 2. Weights W(R(i)) of the Various Rumer Blocks for $C_{2n}H_{2n+2}$ Polyenes at the VBSCF(AO-C), VBSCF(BDO-C), and VBSCF(OEO-C) Levels.[a]

	W(R(0))			W(R(1))			W(R(2))			W(R(3))		
	AO-C	BDO-C	OEO-C	AO-C	BDO-C	OEO-C	AO-C	BDO-C	OEO-C	AO-C	BDO-C	OEO-C
C_4H_6	0.877	0.871	0.905	0.123	0.129	0.095	–	–	–	–	–	–
C_6H_8	0.748	0.758	0.806	0.246	0.250	0.187	0.006	−0.008[c]	0.007	–	–	–
C_8H_{10}	0.629	0.588	0.712	0.343	0.356	0.265	0.028	0.06	0.023	0.000	−0.004[c]	0.000
$C_{10}H_{12}$	0.525	**0.473**[b]	0.627	0.409	0.453	0.325	0.065	0.09	0.047	0.001	−0.024[c]	0.001
$C_{12}H_{14}$	**0.435**[b]		0.550	0.446		0.369	0.112		0.077	0.007		0.004
$C_{14}H_{16}$	0.360		**0.482**[b]	0.460		0.398	0.163		0.111	0.017		0.010
$C_{16}H_{18}$	0.296		0.423	0.456		0.414	0.212		0.144	0.034		0.018
$C_{18}H_{20}$	0.261			0.415			0.248			0.075		

[a]These weights were determined for the B3LYP optimized geometries. Using MP2 optimized geometries basically leads to very similar weights (see Tables S1−S5). [b]The W(R(0)) values in bold are the first ones that fall below W(R(0)) = 0.5. [c]Small negative values of Coulson-Chirgwin weights occasionally occur in VB calculations for unimportant structures. These are regarded as zeros.

increases slightly toward the center of the polyene. On the other hand, the lengths of the "single" C−C bonds gets a bit shorter as we move toward the center of the polyene. We note that these trends occur also in some carotenoids (e.g., in desmethyl β carotene).[50]

The impression given by the optimized geometries is that we are indeed dealing with a localized system, described approximately by the classical Rumer structure, R(0). So, let us inspect the VB wave functions of these polyenes and see if indeed they are dominated by the R(0) fundamental structure. Table 2 shows weights for the Rumer structures' blocks for various polyenes at the VBSCF(AO-C), VBSCF(BDO-C), and VBSCF(OEO-C) levels.

A surprise, the weight of the fundamental structure, W(R(0)), decreases quite fast. At some polyene size, while W(R(0)) is still the single largest weight, nevertheless, the combined weights of the first excited Rumer block, $\boldsymbol{R}$(1), exceed W(R(0)). The exact polyene size where this crossover occurs depends on the VBSCF level, but the trend is independent of the VBSCF level. Moreover, it is seen that as the polyene grows it develops a substantial tetra-radicaloid behavior and even some hexa-radicaloid (due to mixing of $\boldsymbol{R}$(2) block Rumers), though to a much lesser extent. Indeed, a very delocalized diradicaloid description of polyenes emerges from VB theory.

While the trend is clear and common for the three AO types, the reader will notice a substantial difference (up to a factor of 2) in the weights of specific diradicaloid and polyradicaloid structures calculated by the two better levels (OEO-C and BDO-C). These differences might reflect the fact that due to the delocalization tails in the BDO and OEO orbitals, each spin coupling between two semilocalized orbitals embed in addition to the main bond coupling also minor bond couplings. But this remains to be explained.

5. DISCUSSION

Let us see if we can reconcile the two seemingly diametrically opposite pictures of bond localization vs a delocalized wave function.

5.1. Why is Bond Alternation Conserved Despite the Highly Delocalized Nature of the Polyene? We begin with the structural aspect. It is reasonable to postulate that the actual bond length associated with the full wave function are averages over the bond lengths associated with component VB structures[51] weighted in the same way that they contribute to the full wave function. eq 8 expresses this idea:

$$R_i = \sum_{Ks} W_{Ks}\bar{R}_s + \sum_{Kl} W_{Kl}\bar{R}_l \quad (8)$$

Here, $\bar{R}_s$and $\bar{R}_l$ are the average short and long bond lengths obtained from the B3LYP optimized geometries. The first summation runs over all Rumer structures in which the ith-bond is a short bond ($\bar{R}_s$), while the second over those long i-bonds ($\bar{R}_l$). Table S2 exemplifies the details of the predictions for hexatriene, which has five Rumer structures.

The predictions of the equation for C_8H_{10} and $C_{10}H_{12}$ are shown in Figure 3 alongside the optimized geometries. It is

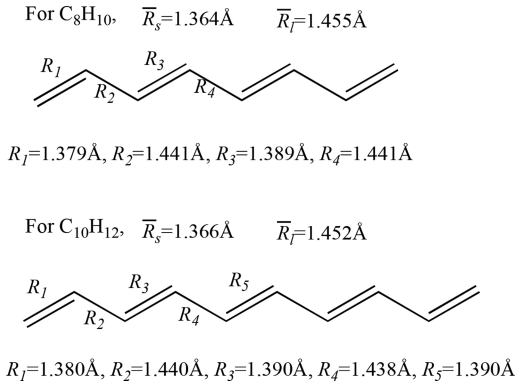

Figure 3. Optimized C−C bond lengths (below the structures) and predicted ones based on eq 8 (above the structures) for C_8H_{10} and $C_{14}H_{16}$.

seen that the equation predicts reasonably well the bond alternation, and as such, it shows that a highly delocalized wave function gives rise to a geometry that looks as though the double and single bonds are localized as in the fundamental Rumer structure. The reason for this behavior is elucidated by the data in Table 2, which shows that except for R(0), the wave function is dominated by the R(1,j) structures of the $\boldsymbol{R}$(1) block and mostly by the R(1,1) structures that possess $n - 1$ short bonds. Since each R(1,1) structure has a small weight, and since the structure affects only those CC lengths of the four C atoms defining the 1,4-diradical, this mixing has little impact on the overall bond alternation inherent in R(0). Hence, all in all, despite the extensively delocalized wave function, the bond alternation is conserved. But the bond localization does not really reflect the electronic nature of the polyene.

DOI: 10.1021/jacs.7b04410
J. Am. Chem. Soc. 2017, 139, 9302−9316

5.2. Understanding the Behavior of VB Wave Functions of Polyenes. Let us turn now to the nature of the VB wave function and its variation with the polyene's size.

5.2.1. Decay of the Classical Fundamental Rumer Structure. Table 2 reveals clearly that as the polyene grows, the weight of the classical structure $R(0)$ decays rather fast, such that in $C_{10}H_{12}$ or $C_{12}H_{14}$, this weight is overwhelmed by a pack of Rumer structures, dominated by the $\boldsymbol{R}(1)$ block, and specifically by the subset of structures $R(1,1)$, which encompass all 1,4-diradicaloids, separated by a single π bond. Hence, even though $W(R(0))$ is the single largest weight for an individual Rumer structure, considering the collective weight of the $R(1,1)$ sub-block, we conclude that the polyene is described approximately as a delocalized diradicaloid species rather than a classical type as $R(0)$. This feature does not depend greatly on the degree of bond alternation; it is a fundamental feature of the wave function. Let us proceed now to model this decay of $W(R(0))$.

Scheme 4a shows for butadiene the classical structure, its weight $W_2(0)$ (where 2 indicates here that there are two π bonds in $R(0)$ of butadiene), and the corresponding 1,4-diradicaloid's weight $W_{DR}(1,1)$, at the VBSCF(AO-C) level. Since for higher polyenes the dominant diradicaloid sub-block is $R(1,1)$, which involves only 1,4-diradicaloids, the weight of the classical structure $W_n(0)$ for higher polyene of the general formula $C_{2n}H_{2n+2}$ will be the product of the elementary weights of all the "butadienic fragments" that can be drawn for the polyene. As illustrated in Scheme 4b, this number is $n-1$. Thus, we can write

$$W_n(0) = [W_2(0)]^{(n-1)} \tag{9}$$

Since $W_2(0) = 0.877$, which is very close to $3^{1/2}/2$, we use $W_2(0) = 3^{1/2}/2$ in eq 9 and calculate the weights for the various polyenes. The so calculated $W_n(0)$ values are plotted in Figure 4 against n, alongside with the VBSCF values for the three AO types.

The closeness of the modeled and VBSCF sets of values is satisfactory, considering that we neglected all other diradicaloids contributions in deriving eq 9. This just underscores the conclusion that the $R(1,1)$ sub-block of Rumer structures is the main one that mixes with the fundamental classical structure $R(0)$.

Note the fast decay, in Figure 4, of the weight $W_n(0)$ as the polyene grows. In all the sub-Figures of Figure 4, the actual VBSCF weights decay faster than the ones predicted by eq 9. This is because the actual calculations include the effect of all the $\boldsymbol{R}(k)$ blocks (see Table 2), whereas eq 9 uses the $R(1,1)$ sub-block.

5.2.2. Hierarchy of the Rumer Structures in the R(1,j) Sub-Block. As we argued, the major diradicaloid structures that mix into the classical fundamental Rumer $R(0)$ are the $R(1,1)$ structures, while other $R(1,j)$, $j > 1$, structures mix less and less as the number of intervening bonds between the diradical increases. Higher Rumer blocks mix even less. So, let us focus on $R(1,j)$, $j \geq 1$, Rumer structures, and see their behavior in the total wave function.

Scheme 5 depicts these structures for three polyenes as examples of the general behavior, while Figure 5 plots the weights $W(R(1,j))$ as a function of j which is the number of intervening double bonds between the diradicaloid ends. It is seen that these weights decay very fast as j increases, and the lowest weight is always for the $R(1,n-1)$ structure, the end-to-end diradical. The weight of this structure further decreases as the polyene grows, becoming 0.030, 0.012, and 0.005 for C_6H_8, C_8H_{10}, and $C_{10}H_{12}$, respectively. As we argued in the section on

Scheme 4. (a) Weights $W_2(0)$ of the Classical Structure and the 1,4-Diradicaloid One $W_{DR}(0)$ for Butadiene at the VBSCF(AO-C) level and (b) Butadienic Units that Can Generate 1,4-Diradicaloids for C_6H_8, C_8H_{10}, and $C_{2n}H_{2n+2}$ are Circled

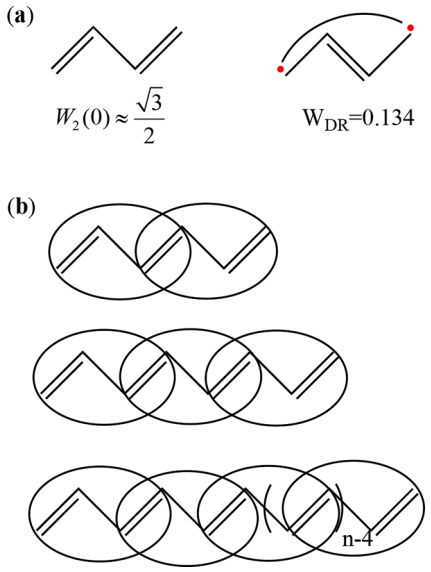

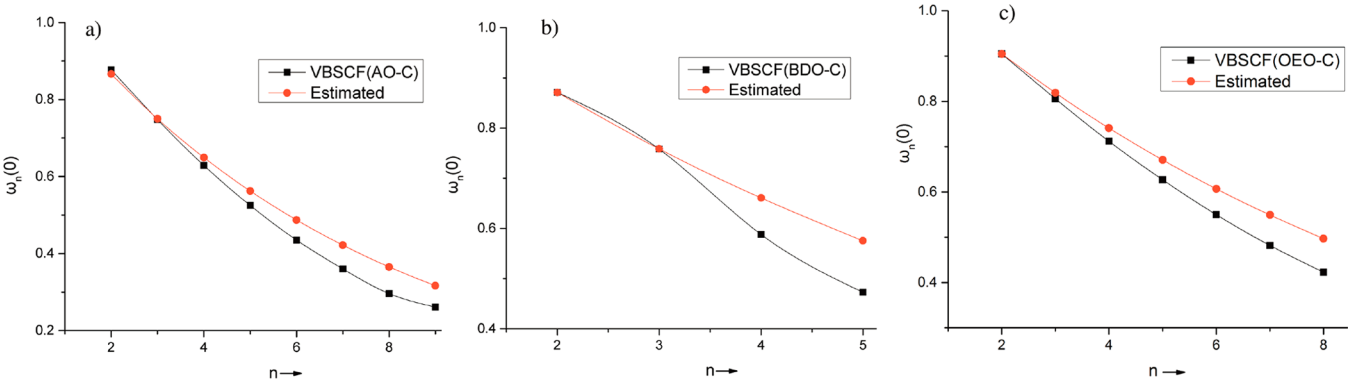

Figure 4. Plots of predicted (eq 9) and VBSCF Computed Weights $W_n(0)$ of the Classical Fundamental Rumer Structure, $R(0)$, Against n, for Polyenes, $C_{2n}H_{2n+2}$: (a) VBSCF(AO-C), (b) VBSCF(BDO-C), and (c) VBSCF(OEO-C).

DOI: 10.1021/jacs.7b04410
J. Am. Chem. Soc. 2017, 139, 9302−9316

Scheme 5. $R(1,j)$ structures for C_6H_8, C_8H_{10}, and $C_{10}H_{12}$

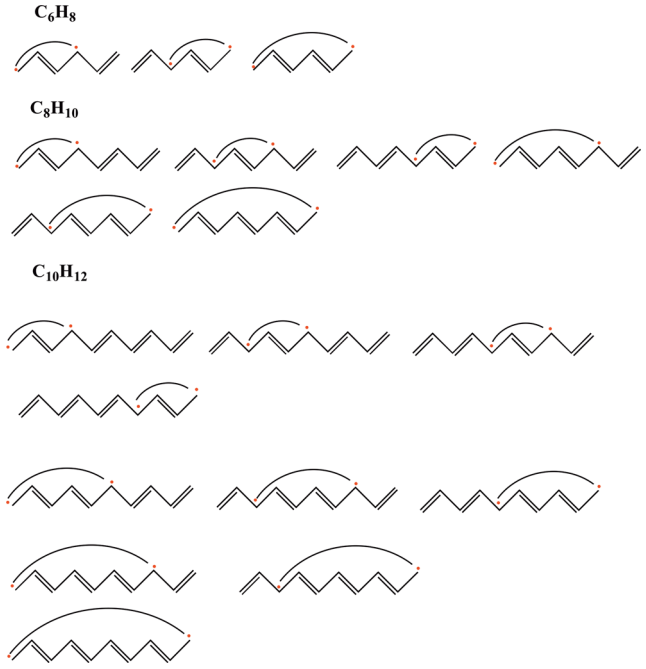

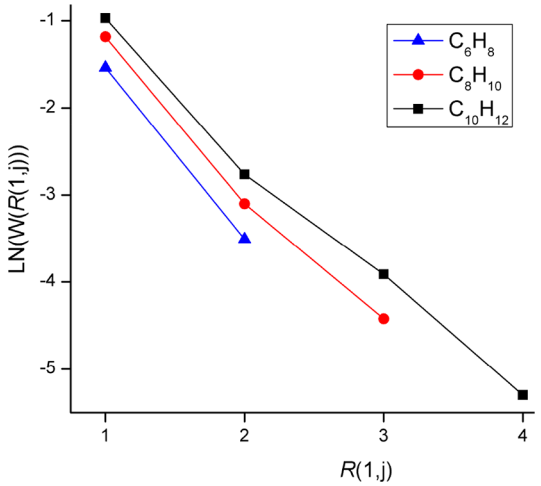

Figure 5. Natural logarithms ln(W(R(1,j)) of the weights for the $R(1,j)$ structures in the full VBSCF(BDO-C) wave function for C_6H_8, C_8H_{10}, and $C_{10}H_{12}$.

perturbation theory, as the number of intervening bonds, j, increases, the corresponding reduced matrix element β_{j0} [with regard to the mixing with $R(0)$] decreases, while the energy gap $(E_0 - E_j)$ relative to $R(0)$ increases. Consequently, the mixing coefficient given by $C_j = \beta_{0j}/(E_0 - E_j)$ decays very fast.

5.3. Delocalization Energy of Polyenes: Are the π–π Interactions Net Stabilizing? On the basis of the above considerations, the VBSCF wave function may be written in the following approximate manner, dropping the normalization constant:

$$\Psi_{\mathrm{VBSCF}} \approx \Phi_{R(0)} + C_{1,1}\Phi_{R(1,1)} + C_{1,j}\Phi_{R(1,j)} \tag{10}$$

Here, $\Phi_{R(0)}$ is the VBSCF wave function for the classical Rumer structure $R(0)$, $\Phi_{R(1,1)}$ is the multistructure wave function of the various $R(1,1)$ first-block Rumers, while $\Phi_{R(1,j)}$ is the collective wave function of the other Rumers in the first block with more than one double bond intervening between the diradical ends. The C's are the coefficients of the corresponding multistructure wave function, such that $|C_{1,1}| > |C_{1,j}|$ as argued above and as seen from Figure 5. This is further demonstrated in Table 3,

Table 3. Comparison of VBSCF(BDO-C)/D95V Energies for the Full VBSCF Rumer Set and for Truncated Ones Using Only $R(0)$ and $R(1,1)$ Rumer Structures (in a.u.)

	VBSCF(AO-C)		VBSCF(BDO-C)	
$C_{2n}H_{2n+2}$	$E[R(0)+R(1,1)]$	E(full)	$E[R(0)+R(1,1)]$	E(full)
C_4H_6	−154.8648	−154.8648	−154.9233	−154.9233
C_6H_8	−231.7173	−231.7173	−231.8195	−231.8200
C_8H_{10}	−308.5696	−308.5697	−308.7080	−308.7111
$C_{10}H_{12}$	−385.4217	−385.4220	−385.5957	−385.6019
$C_{12}H_{14}$	−462.2735	−462.2743	−462.4828	
$C_{14}H_{16}$	−539.1251	−539.1266		
$C_{16}H_{18}$	−615.9762	−615.9788		
$C_{18}H_{20}$	−692.8271	−692.8310		

which shows that $E[R(0) + R(1,1)]$ of the wave function obtained from mixing of the $R(1,1)$ structures into $R(0)$, yields VBSCF energies very close to the full VBSCF wave function. The remaining $R(1,j)$, $j > 1$, structures make a significantly smaller contribution to the total energy.

It is clear therefore that we may express the ground state's wave function in the following good approximation:

$$\Psi_{\mathrm{VBSCF}} \approx \Phi_{R(0)} + \sum_j [C_j\Phi_{R(1,j)}](j = 1, 2, \cdots, n-1) \tag{11}$$

To be on the safe side, we include here all the $\boldsymbol{R}(1)$-block structures, given by $R(1,j)$, $j = 1,2,...,n-1$, where j runs over all the Rumer structures of block 1, while the C_j terms are individual coefficients $C_j = \beta_{0j}/(E_0 - E_j)$. If we simply use the VBSCF coefficient, we can then calculate the delocalization energy (ΔE_{del}) of the polyene obtained by mixing the $\boldsymbol{R}(1)$ Rumer structures into $\boldsymbol{R}(0)$ based on the following perturbation expression derived from eq 7:

$$\Delta E_{\mathrm{del}} = \sum_j [C_j\beta_{0,j}] \tag{12}$$

Table 4 shows the delocalization energies for the polyene series from C_4H_6 to $C_{14}H_{16}$. It is seen that the perturbation expression provides a very good approximation to the total delocalization energies calculated by the full VBSCF wave function. As the polyene grows, the deviation from the computed ΔE_{del} increases somewhat. The deviations are rather small, and Table 4 already makes it clear that the model based on eq 12 is quite successful and needs no further complications (for more information see Tables S4–S5).

To further explore the utility of the model, we show in Figure 6 (panels a and b) plots of the $\Delta E_{\mathrm{del}}/n$ values versus the number of the short π-bonds, n, in the classical polyene structure, for the VBSCF(BDO-C) computed values. Figure 6a shows the plots for $\Delta E_{\mathrm{del\text{-}VBSCF}}$ and eq 12 based $\Delta E_{\mathrm{del\text{-}Pert}}$ using the D95V basis set and Figure 6b the same quantities for STO-6G, where data for the larger polyenes is presented. In all the plots in Figure 6, there is an excellent linear correlation ($r^2 > 0.997$), which is expressed in eq 13:

$$\Delta E_{\mathrm{del}}/n = a + be^{[-cn]} \tag{13}$$

DOI: 10.1021/jacs.7b04410
J. Am. Chem. Soc. 2017, 139, 9302–9316

Table 4. ΔE_{del} Values (in kcal mol^{-1}) for $C_{2n}H_{2n+2}$ (n = 2−7) Obtained from VBSCF(BDO-C)/D95V Calculations As Well As from the Perturbation Expression (eq 12)

molecule	C_4H_6	C_6H_8	C_8H_{10}	$C_{10}H_{12}$	$C_{12}H_{14}$	$C_{14}H_{16}$
$\Delta E_{del\text{-}VBSCF}$[a]	−5.90	−13.30	−20.90	−28.30	−35.58	−42.48
$\Delta E_{del\text{-}Pert}$	−5.95	−13.18	−20.62	−28.24	−36.41	−45.05

[a]These are VBSCF values relative to the corresponding $E(R(0))$.

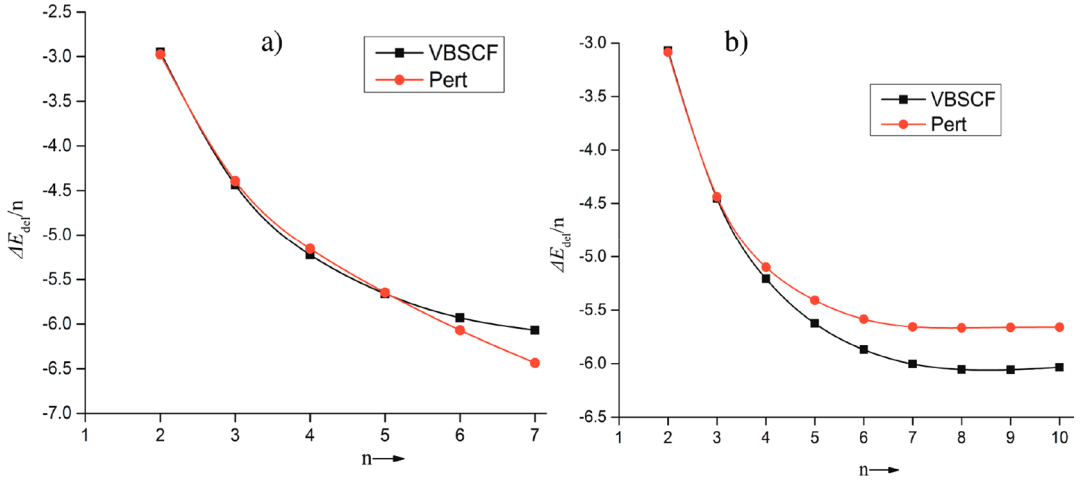

Figure 6. Plots of the delocalization energies, ΔE_{del} calculated with VBSCF and predicted using perturbation theory vs the poylene size n: (a) $\Delta E_{del\text{-}VBSCF}/n$ using VBSCF/D95V and corresponding $\Delta E_{del\text{-}Pert}/n$. (b) $\Delta E_{del\text{-}VBSCF}/n$ using VBSCF/STO-6G and corresponding $\Delta E_{del\text{-}Pert}/n$.

As n goes to infinity, the expression is simplified to a linear function of the polyene size n:

$$\Delta E_{del} = a \times n \tag{14}$$

where a is a constant energy increment per one π bond. For example, for Figure 6 (panels a and b), these expressions become (in kcal mol^{-1}):

$$\Delta E_{del-VBSCF} = -6.331 \times n \tag{15a}$$

$$\Delta E_{del-Pert} = -6.869 \times n \tag{15b}$$

The expressions for the STO-6G data in Figure 6b are very similar ($\Delta E_{del\text{-}VBSCF} = -6.106 \times n$ and $\Delta E_{del\text{-}Pert} = -5.679 \times n$) despite the different basis sets. Furthermore, in each case, the VBSCF calculated and perturbation expressions are close and they show that the delocalization energy of long polyenes is a linear function of the number of double bonds n in the fundamental valence structure. Thus, despite the extensively delocalized nature of the polyene, the total conjugation energy between its double bonds is additive, or size-extensive, and made up from 6 to 7 kcal mol^{-1} contributions per one double-bond (with D95V and STO-6G). Note that for a finite polyene, there are $n - 1$ conjugative interactions between double bonds, so a single conjugative interaction will be given by $a \times n/(n - 1)$, while for an infinitely long polyene, it would be simply a, which is 6−7 kcal mol^{-1}.

Thus, for an infinitely long polyene, the delocalization energy between two π bonds was just determined to be $\Delta E_{del} = -(6-7)$ kcal mol^{-1}. To assess this quantity, we may compare it to the previously determined conjugative interaction in butadiene. The Kollmar value[11] of $\Delta E_{del} = -9.7$ kcal mol^{-1} and the more recent BLW value[13] of $\Delta E_{del} = -12.6$ kcal mol^{-1} are higher. This is partly due to differences in the butadiene bond lengths in the three studies and partly due to the different methodologies. Therefore, to ascertain the dependence of ΔE_{del} for butadiene on the VBSCF level, we used the VBSCF with the full-space of structures (covalent and ionic), as well as VBSCF(OEO-C), and we also varied the basis set to 6-31G* and cc-pVTZ. The so resulting ΔE_{del} ranges between −5.9 and −9.7 kcal mol^{-1} (see Table S4B).

5.3.1. Are the π−π Interactions in Polyenes Net Stabilizing? We are now in a position to address this question. Thus, for an infinitely long polyene, the delocalization energy between two π bonds was just determined to be −(6−10) kcal mol^{-1}. On the other hand, we recall from Figure 2 (see the inset there) that the destabilization of the two conjugated π-bonds in the classical Rumer structure is 0.5λ, where λ is the strength of a π interaction, which is distance-dependent.[3] For an average distance of the long C−C (1.45 Å), where λ = 45.0/33.7 kcal mol^{-1} (depending on usage of the ground/triplet states as reference states. See Section 1 eqs S9a and S9b), the repulsive interaction is 22.5/17.0 kcal mol^{-1}. The lower value is of a similar order as the corresponding BLW value of 16.9 kcal mol^{-1} determined from a model B_4H_2,[13] and the repulsive interference/delocalization value of 18.4 kcal mol^{-1} determined relative to the QCS reference (analogous to **1**).[17a]

Still another method to determine the Pauli repulsion term is by direct use of the present VBSCF calculations. Thus, in a uniform geometry where all CC distances are identical to the optimized central CC bond of butadiene (Table 1), the energy gap between the two Rumer structures of butadiene (see page S8) is 3/2(λ) (where $\lambda = \lambda'$; see Figure 2). This leads to values of 0.5λ = 13.6/18.7 kcal mol^{-1}, for VBSCF(AO-C)/VBSCF-(BDO-C), respectively. The range of values is shown in Figure 7. Thus, even if we take the highest absolute value for the delocalization energy and the lowest one for the repulsive energy in Figure 7, we still reach the conclusion that the repulsive $\pi-\pi$ interaction, $\Delta E_{rep}^{\pi-\pi}$, is larger than the conjugative interaction, ΔE_{del}, in accord with previous conclusions.[7,17] This judgment reflects the fact that ΔE_{del} is a

DOI: 10.1021/jacs.7b04410
J. Am. Chem. Soc. 2017, 139, 9302−9316

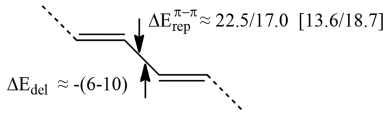

Figure 7. Delocalization energy (stabilizing interaction) and the Pauli repulsive $\pi-\pi$ interaction between two π bonds in a long polyene (in kcal mol^{-1}). The repulsive interactions out of brackets are estimated based on the semiempirical VBSCF study (ref 3), while those in square brackets are estimated directly from the present VBSCF calculations where, here, the values refer to (AO-C)/(BDO-C), respectively.

second-order effect, while the Pauli repulsion is a first-order and hence, a larger term.

The above conclusion may seem controversial at first sight. How can a polyene have a repulsive $\pi-\pi$ interaction and still remain planar? While we have not dealt here with the rotational barrier issue, which for us is a digression, others did.[17,52,53] The rotational barrier is not a measure of the delocalization energy but is rather a net outcome of a conglomerate of many factors. Thus, both the planar (*s-trans*) ground state and the perpendicular transition state (TS) for rotation involve a mixture of conjugative stabilizing interactions along with Pauli-repulsive interactions of various bonds, as well as σ_{CC}-compression effects.[52,53] In 1980, Daudey and Malrieu et al.[52] showed that the various hyperconjugative interactions (σ_{CC}-π^*, σ_{CH}-π^*, $\pi-\sigma^*_{CH}$, and $\pi-\sigma^*_{CC}$) in the perpendicular TS are responsible for the fact that the central C−C bond remains short (1.499 Å). And, furthermore, the total hyperconjugative stabilization of the TS (−8.9 kcal mol^{-1}) is almost as stabilizing as the π-delocalization energy (−10.4 kcal mol^{-1}) in the planar *s-trans* structure of butadiene. This shows that the rotational barrier reflects the somewhat greater Pauli repulsions (and possibly others) in the TS. Using the same technique as Mo et al.,[53b] we verified the conclusion of Daudey and Malrieu for butadiene.[52] Furthermore, we found that strictly π-localized structure for the planar ground state exhibits a rotational barrier that is virtually as large as that computed for the delocalized species (∼7−8 kcal mol^{-1}). Thus, the rotational barrier in butadiene originates in augmented Pauli repulsion in the rotational TS. This is reminiscent of the rotational barrier in ethane, which is determined mostly by the excessive Pauli repulsion in the eclipsed conformer, while the hyperconjugative interactions are almost identical for the two conformers.[53d]

5.4. Comparison of the Ground and the First Excited Covalent States of Polyenes. As we mentioned in the introduction, there are two important covalent excited states of polyenes. The lowest energy of these is 2^1A_g having the same symmetry as the ground state 1^1A_g. The second excited state is $1^1B_u^-$. To illustrate the origins of these states, consider the five Rumer structures in Figure 8a for C_6H_8. These are the fundamental structure $\boldsymbol{R}(0)$, three $\boldsymbol{R}(1)$ structures, and a single $\boldsymbol{R}(2)$ structure.

Figure 8b classifies the symmetry of these Rumer structures. It is seen that $R(0)$, $R(1,2)$, and $R(2)$ all belong to the A_g irreducible representation, while $R(1,1)$ and $R(1,1)'$ are not symmetry adapted. As shown in the right-hand side of Figure 8b, taking positive and negative linear combinations creates $R(1,1)^+$, which transforms as A_g, and $R(1,1)^-$ which transforms as B_u^-. However, in VB these combinations involve also a matrix element between the two structures that cause the energies of the combinations to split, as shown in Figure 8b.

The symmetry classification simplifies the constitutions of the states. Figure 8c shows the mixing diagram that generates

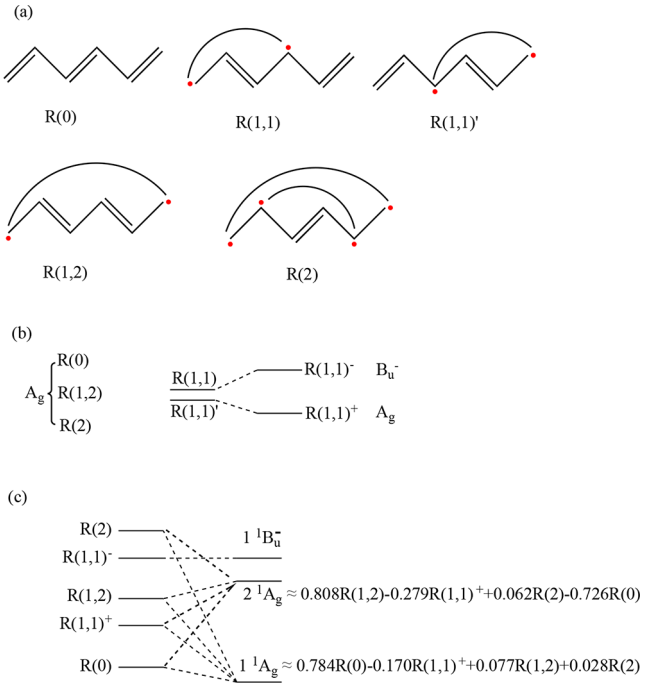

Figure 8. Generation of the covalent states, 1^1A_g, 2^1A_g, and $1^1B_u^-$ for C_6H_8. (a) The corresponding Rumer structures. (b) Symmetry classification of the structures and of the $R(1,1)^{+/-}$ combinations. (c) Structure mixing diagram leading to the corresponding states. The values of the coefficients are taken from the VBSCF(BDO-C)/D95V calculations.

the ground and two excited states. It is apparent that the $1^1B_u^-$ state is identical to the B_u^- combination of $R(1,1)$ and $R(1,1)'$. On the other hand, the ^1A_g states will arise from a more complex mixing of all the Rumer structures and combinations that transform as A_g. As should be clear by now, the ground state 1^1A_g is generated by the fundamental Rumer structure $R(0)$ mixed in bonding fashion with the $R(1,1)^+$ combination and less so [due to the reduced matrix element effect; see above] $R(1,2)$ and even smaller contribution from $R(2)$. On the other hand, 2^1A_g is dominated by end-to-end diradicaloid $R(1,2)$ mixed in an antibonding fashion with $R(1,1)^+$ and a bonding combination of $R(2)$ (see Table S7, equations S12−S13). These are general features of these states, which will not be altered as the polyene gets longer, just becoming more complex because of the many Rumer structures (Equations S12−S14). More details can be found in Tables S6 and S7 and Scheme S6.

5.5. Manifestations of the Diradical or Diradicaloid Nature of Polyenes. Does the significant collective-diradical character of polyenes, emerging so clearly in our VB study, manifest itself in physical and chemical properties? There is intense interest in the diradical character of formally closed shell organic molecules. One reason is of course intellectual,[37a,b,54] while another is practical.[37c−f,h−j,55−59] Thus, as shown in Scheme 6, oligomers of polyacenes (**4**), quinodimethanes (**5**), and various derivatives of these molecules, as well as 1,3-dipoles (**6** and **7**), are consistently described as diradicaloids, diradicals, and sometimes as polyradicals.[37a] Synthetic derivatives of **4** and **5** exhibit large nonlinear optical properties, unusual magnetic and optical properties, and they serve as organic field effect transistors.[37d−f,h−j] Diradical character is an essential feature of candidates for the fascinating phenomenon

DOI: 10.1021/jacs.7b04410
J. Am. Chem. Soc. 2017, 139, 9302−9316

Scheme 6. Molecules with Diradical Characters, 4−7

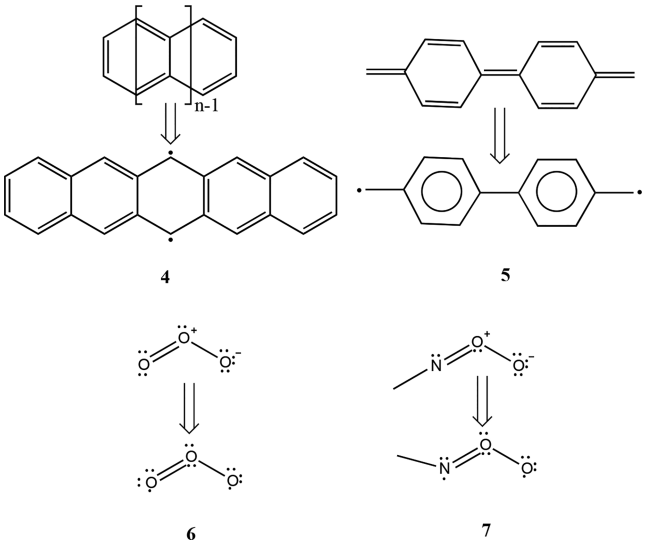

of singlet fission.[55] Other consequences of the 1,3-dipolar reagents are their reactivity patterns.[54] Recently, Braida and Hiberty[57] showed that the barriers for cycloaddition of a variety of 1,3-dipoles to ethylene correlate with the inverse of the diradical character of the 1,3-dipoles. The dimerization of the parent quinodimethane to [2,2]paracyclophane may also be ascribed to its diradical character, as well as to the aromatization of two rings. Transmission of current across single molecules reflects highly mobile electrons and may be associated with increased diradical character in a conducting molecule or oligomer/polymer.[58]

What about reactivity? The relationship of diradical reactivity to that of radicals needs to be delineated carefully and with proper cognizance of spin and spatial symmetry. This will be done in more detail in a future contribution by some of us; here we just mention the problems that arise.

The reactivity of simple radicals (H, CH_3) is extraordinary: they dimerize in a shot, unless there be steric impediments; they add to olefins and abstract hydrogen and chlorine atoms with low activation barriers. True diradicals are more complex. What do we mean by true diradicals? We have in mind trimethylenemethane or 1,3-meta-quinodimethane. The diradical nature of these molecules arises from their electronic structure: two electrons in two degenerate or nearly degenerate orbitals. Of the six resulting microstates, a triplet and three singlets, two compete for being the ground state of the molecule, the open-shell triplet and, generally, an open-shell or closed shell singlet. The reactivity of these two states is very different; this is what a further study will take apart.

Diradicaloids are near diradicals: they have a ground state singlet (often with strong configurational mixing) and a relatively low-lying triplet. Various measures of diradicaloid character have been proposed.[60] The polyenes fall into the class of diradicaloids, especially as they become longer. The antibonding nature revealed in Figure 1d for the OEOs of 1,4-diradicaloids makes them particularly interesting despite the fact that the entire pack of diradicaloid-Rumer structures delocalizes the 1,4-diradicals over the polyenes. Thus, the polyene's diradical character may be responsible for their enhanced reactivity relative to isolated double bonds. Polyenes are known also to be photoconductors with small energy gaps, and this property may also reflect the high diradical character.

One should be cautious to attribute too many physical manifestations to the diradical character of polyenes. First, the fundamental $R(0)$ structure maintains the largest individual weight, while the diradicaloid structures undergo delocalization, and their mutual mixing imparts stability to the pack. Second, along with the change of the diradical character other properties of the molecule change too. For example, a high diradical character necessarily means that there is a very low-lying triplet state.[60c,h] Indeed, our B3LYP/D95V calculations show that for $C_{20}H_{22}$ and $C_{28}H_{30}$, the singlet−triplet excitations are 15.5 kcal mol^{-1} and 11.1 kcal mol^{-1}, respectively (for the way the singlet−triplet excitation evolves as polyenes grow longer, see Table S8). As such, in the case of reactivity, for instance cycloaddition reactions with polyenes, the reaction barriers are proportional to the singlet-to-triplet excitation energy of the reacting molecules. A low value will result in a low barrier, indeed (see ref 23, pp. 116−192).[61−63] These very low singlet−triplet excitation values will make the long polyenes very susceptible to cross-linking. Similarly, the tendency of polyenes (starting with butadiene) to exhibit 1,4-reactivity (which Thiele ascribed in 1899 to residual affinities in these sites) might be attributed to the 1,4-diradicaloid characters of the molecules. But using VB modeling of the barrier (see ref 23, Ch. 6),[23,61−63] the 1,4 reactivity actually derives from the triplet state of the molecule, which is purely a 1,4-triplet diradical. As we already stated, these properties, a low-lying triplet state, high diradical character, are not separate properties. As most clearly shown by Nakano, they are intimately connected with each other.[60c]

Considering all the above, it is not clear if the diradicaloid character of polyenes is a physical observable property as in real diradicals. Thus, on the one hand, the VB wave function shows vividly how the diradical character increases exponentially with the growth of the polyene and that this affects the polyene properties and its reactivity. On the other hand, the diradicaloid structures are highly delocalized and may be considered as the way VB theory delocalizes the double bonds, which are localized in the fundamental structure.

■ CONCLUSIONS

We asked at the outset the following question. Are polyenes localized or delocalized? To respond to this question, we used VBSCF calculations and modeling of polyenes, $C_{2n}H_{2n+2}$. The theoretical treatment shows that the polyenes may be described primarily by a shifting 1,4-diradicaloid character, which increases as the chain length increases. Around n = 5, the wave function of the polyene starts to be dominated by a collection of 1,4-diradicaloid structures, while the fundamental pristine structure with alternating double and single bonds (**1**) decays quite fast (Figure 4) and becomes minor relative to the diradicaloid pack. Nevertheless, it is this wave function that predicts in a simple fashion that the polyene will exhibit alternating short/long CC bonds like the fundamental structure **1**. Furthermore, despite the decay of **1**, it remains the single structure with the largest weight among all the individual structures. The mixing of all the 1,4-diradicaloid structures into **1** follows perturbation theory rules, with the result that the delocalization energy due to this mixing is additive and behaves as a linear function of the number of the double bonds (eq 15b), n, namely, $\Delta E_{del} = -6.9 \times n$ (kcal mol^{-1}), where for infinitely long polyenes the 6.9 kcal mol^{-1} is the conjugation energy between double bonds (see Table S4B for the value with OEO). Furthermore, in accord with previous conclu-

DOI: 10.1021/jacs.7b04410
J. Am. Chem. Soc. 2017, 139, 9302−9316

sions,[5,13,17] the VB modeling shows that while π conjugation stabilizes structure **1**, nonetheless, this relatively weak delocalization energy is insufficient to overcome the first-order Pauli repulsive terms between two adjacent π bonds. Even so, polyenes can be and are planar.[17] Thus, for butadiene the nonplanar rotational-transition-state (RTS) has a virtually identical delocalization energy[52,53] as the planar ground state, and the rotational barrier reflects larger repulsive interactions in the perpendicular RTS.

Several potential manifestations of this diradicaloid character are discussed, for example, decreasing singlet−triplet energy gaps (e.g., 11.1 kcal mol^{-1} for $C_{28}H_{30}$ in Table S8) and consequently increasing reactivity,[61−63] increasing photoconductivity, etc., as the polyene gets longer. Nevertheless, it is concluded that this diradicaloid character is clearly not as well-defined a physical property as in real diradicals.

Thus, we went full circle to realize that our philosophical question may not be strictly resolved. The localized/delocalized properties of polyenes seem to define a "chemical complementarity/duality principle". Once we localize the bonds as in **1**, a duality principle steps in and causes indefinite location of the bonds. A similar finding[64] was reported for hexagonal X_6 species (X = H, Li, and CH), wherein the respective MO-based wave functions of the Kekulé structures or the delocalized states were expanded to their covalent and ionic structures. For these hexagons, it was observed that while each local X−X bond was primarily covalent ($W_{COV} \approx 0.75$), the covalent structure of the whole X_6 species decayed as an exponential function of W_{COV}. This decay was much faster in the delocalized hexagonal species, where the VB projected wave function was dominated by ionic structures (monoionics and higher), even though the local bonds remained covalent. This duality of the molecular wave function is a ubiquitous and will remain a beguiling phenomenon.

■ ASSOCIATED CONTENT

Supporting Information

The Supporting Information is available free of charge on the ACS Publications website at DOI: 10.1021/jacs.7b04410.

Bond lengths and XYZ coordinates of polyenes calculated by B3LYP, BH&HLYP, and MP2 methods, Rumer structures, overlaps and weights of Rumer structures, valence bond bond orders, explanations semiempirical valence bond related data, and B3LYP calculated singlet−triplet excitation energies of polytenes (PDF)

■ AUTHOR INFORMATION

Corresponding Authors

*sason.shaik@gmail.com
*weiwu@xmu.edu.cn
*rh34@cornell.edu

ORCID

Roald Hoffmann: 0000-0001-5369-6046
Yuta Tsuji: 0000-0003-4224-4532
Sason Shaik: 0000-0001-7643-9421

Notes

The authors declare no competing financial interest.

■ ACKNOWLEDGMENTS

The research in HU was supported by the ISF (ISF grant 1183/13) and in XMU by the NSFC (Grants 21290193 and 21673186). S.S. and D.D. thank Prof. Y. Mo for advice on BLW calculations. The Cornell work was supported by the National Science Foundation through Grant CHE-1305872. We thank Tao Zeng for some useful comments. All the authors are thankful to Dr. Jilai Li from the Technical University of Berlin for drawing the beautiful TOC, designed by the authors.

■ REFERENCES

(1) For general reviews on aspects of polyenes, see: (a) Kertesz, M.; Choi, C. H.; Yang, S. *Chem. Rev.* **2005**, *105*, 3448−3481. (b) Orlandi, G.; Zerbetto, F.; Zgierski, M. Z. *Chem. Rev.* **1991**, *91*, 867−891.

(2) Craig, N. C.; Groner, P.; McKean, D. C. *J. Phys. Chem. A* **2006**, *110*, 7461−7469.

(3) Wu, W.; Danovich, D.; Shurki, A.; Shaik, S. *J. Phys. Chem. A* **2000**, *104*, 8744−8758.

(4) Hiberty, P. C.; Danovich, D.; Shurki, A.; Shaik, S. *J. Am. Chem. Soc.* **1995**, *117*, 7760−7768 In this method, the π-nonbonded structure of a double bond is obtained by unpairing the electrons of the bond. By optimizing the geometry of the single determinant that has opposite spins (so called quasiclassical state), one gets a C−C distance of 1.44 Å for ethylene. A similar strategy for benzene generates a spin-alternant determinant for the π-electronic component, and its optimization leads to C−C distances of 1.44 Å..

(5) (a) Dewar, M. J. S.; Gleicher, G. J. *J. Am. Chem. Soc.* **1965**, *87*, 692−696. (b) Dewar, M. J. S.; Schmeising, H. N. *Tetrahedron* **1960**, *11*, 96−120. (c) Dewar, M. J. S.; Schmeising, H. N. *Tetrahedron* **1959**, *5*, 166−178.

(6) (a) Kistiakowsky, G. B.; Ruhoff, J. R.; Smith, H. A.; Vaughan, W. E. *J. Am. Chem. Soc.* **1936**, *58*, 146−153. (b) Conant, J. B.; Kistiakowsky, G. B. *Chem. Rev.* **1937**, *20*, 181−194.

(7) Bock, C. W.; George, P.; Trachtman, M. *J. Mol. Struct.: THEOCHEM* **1984**, *109*, 1−16.

(8) Rogers, D. W.; Matsunaga, N.; Zavitsas, A. A.; McLafferty, F. J.; Liebman, J. F. *Org. Lett.* **2003**, *5*, 2373−2375.

(9) Rogers, D. W.; Zavitsas, A. A.; Matsunaga, N. *J. Chem. Educ.* **2010**, *87*, 1357−1359.

(10) Jarowski, P. D.; Wodrich, M. D.; Wannere, C. S.; Schleyer, P.v.R.; Houk, K. N. *J. Am. Chem. Soc.* **2004**, *126*, 15036−15037.

(11) Kollmar, H. *J. Am. Chem. Soc.* **1979**, *101*, 4832−4840.

(12) Cappel, D.; Tüllmann, S.; Krapp, A.; Frenking, G. *Angew. Chem. Int. Ed.* **2005**, *44*, 3617−3620.

(13) Mo, Y.; Zhang, H.; Su, P.; Jarowski, P. D.; Wu, W. *Chem. Science* **2016**, *7*, 5872−5878.

(14) (a) Mo, Y.; Peyerimhoff, S. D. *J. Chem. Phys.* **1998**, *109*, 1687−1697. (b) Mo, Y.; Song, L.; Lin, Y. *J. Phys. Chem. A* **2007**, *111*, 8291−8301.

(15) Schaad, L. J.; Hess, B. A. *Chem. Rev.* **2001**, *101*, 1465−1476.

(16) Shaik, S.; Shurki, A.; Danovich, D.; Hiberty, P. C. *Chem. Rev.* **2001**, *101*, 1501−1539.

(17) (a) Fantuzzi, F.; Cardozo, T. M.; Nascimento, M. A. C. *Phys. Chem. Chem. Phys.* **2012**, *14*, 5479−5488. (b) Cardozo, T. M.; Freitas, G. N.; Nascimento, M. A. C. *J. Phys. Chem. A* **2010**, *114*, 8798−8805. (c) Ruedenberg, K. *Rev. Mod. Phys.* **1962**, *34*, 326.

(18) (a) Hoffmann, R. *Solids and Extended Surfaces: A Chemist's View of Bonding in Extended Structures*; VCH Publishers: New York, NY, 1988. (b) Albright, T. A.; Burdett, J. K.; Whangbo, M. H. *Orbital Interactions in Chemistry*; Wiley-Interscience Publication: New York, NY, 1985.

(19) (a) Kuhn, H. *J. Chem. Phys.* **1949**, *17*, 1198−1212. (b) Bayliss, N. S. *J. Chem. Phys.* **1948**, *16*, 287−292.

(20) (a) Mulliken 1942 on hyperconjugation: Mulliken, R. S. *Rev. Mod. Phys.* **1942**, *14*, 265−274. (b) Woodward, R. B. *J. Am. Chem. Soc.* **1941**, *63*, 1123−1126. (c) Fieser, L. F.; Fieser, M.; Rajagopalan, S. *J. Org. Chem.* **1948**, *13*, 800−806.

DOI: 10.1021/jacs.7b04410
J. Am. Chem. Soc. 2017, 139, 9302−9316

(21) On photoelectron spectroscopy, see: Heilbronner, E.; Bock, H. *The HMO-Model and Its Applications, Basis and Manipulation*; J. Wiley & Sons: London, 1976.
(22) (a) Edmiston, C.; Ruedenberg, K. *Rev. Mod. Phys.* **1963**, *35*, 457−465. (b) Foster, J. M.; Boys, S. F. *Rev. Mod. Phys.* **1960**, *32*, 300−302. (c) Pipek, J.; Mezey, P. G. *J. Chem. Phys.* **1989**, *90*, 4916−4926 Note that these localized orbitals are orthogonal and possess therefore orthogonality tails..
(23) Shaik, S.; Hiberty, P. C. *A Chemist's Guide to Valence Bond Theory*; John Wiley & Sons Inc.: New York, 2008; pp 104−109.
(24) (a) Berry, R. S. *J. Chem. Phys.* **1957**, *26*, 1660−1664. (b) Berry, R. S. *J. Chem. Phys.* **1959**, *30*, 936−941.
(25) Fu*β*, W.; Haas, Y.; Zilberg, S. *Chem. Phys.* **2000**, *259*, 273−295.
(26) Schulten, K.; Karplus, M. *Chem. Phys. Lett.* **1972**, *14*, 305−309.
(27) Simonetta, M.; Gianinetti, E.; Vandoni, I. *J. Chem. Phys.* **1968**, *48*, 1579−1594.
(28) Said, M.; Maynau, D.; Malrieu, J. P.; Garcia Bach, M. A. *J. Am. Chem. Soc.* **1984**, *106*, 571−579. (b) Said, M.; Maynau, D.; Malrieu, J. P. *J. Am. Chem. Soc.* **1984**, *106*, 580−587. (c) Guihery, N.; Ben Amor, N.; Maynau, D.; Malrieu, J. P. *J. Chem. Phys.* **1996**, *104*, 3701−3708.
(29) Li, X.; Paldus. *Int. J. Quantum Chem.* **1999**, *74*, 177−192.
(30) (a) Klein, D. J.; García Bach, M. A. *Phys. Rev. B: Condens. Matter Mater. Phys.* **1979**, *19*, 877−886. (b) Klein, D. J.; Schmalz, T. G.; Seitz, W. A.; Hite, G. E. *Int. J. Quantum Chem.* **1985**, *28*, 707−718.
(31) (a) Nakayama, K.; Nakano, H.; Hirao, K. *Int. J. Quantum Chem.* **1998**, *66*, 157−175. (b) Kawashima, Y.; Nakayama, K.; Nakano, H.; Hirao, K. *Chem. Phys. Lett.* **1997**, *267*, 82−90.
(32) Luo, Y.; Song, L.; Wu, W.; Danovich, D.; Shaik, S. *ChemPhysChem* **2004**, *5*, 515−528.
(33) (a) Hudson, B. S.; Kohler, B. E. *Chem. Phys. Lett.* **1972**, *14*, 299−304. (b) Hudson, B. S.; Kohler, B. E. *J. Chem. Phys.* **1973**, *59*, 4984−5002.
(34) Dunning, T. H., Jr.; Hosteny, R. P.; Shavitt, I. *J. Am. Chem. Soc.* **1973**, *95*, 5067−5068.
(35) (a) van Lenthe, J. H.; Balint-Kurti, G. G. *Chem. Phys. Lett.* **1980**, *76*, 138−142. (b) van Lenthe, J. H.; Balint-Kurti, G. G. *J. Chem. Phys.* **1983**, *78*, 5699−5713. (c) Verbeek, J.; van Lenthe, J. H. *J. Mol. Struct.: THEOCHEM* **1991**, *229*, 115−137.
(36) Rumer, G. *Nachr. Ges. Wiss. Goettingen, Geschaeftliche Mitt.* **1932**, *377*.
(37) (a) Hachmann, J.; Dorando, J. J.; Avilés, M.; Chan, G.K-L. *J. Chem. Phys.* **2007**, *127*, 134309. (b) Trinquier, G.; Malrieu, J.-P. *Chem. - Eur. J.* **2015**, *21*, 814−828. (c) Bendikov, M.; Duong, H. M.; Starkey, K.; Houk, K. N.; Carter, E. A.; Wudl, F. *J. Am. Chem. Soc.* **2004**, *126*, 7416−7417. (d) Sun, Z.; Zeng, Z.; Wu, J. *Acc. Chem. Res.* **2014**, *47*, 2582−2591. (e) Kishi, R.; Ochi, S.; Izumi, S.; Makino, A.; Nagami, T.; Fujiyoshi, J.; Matsushita, N.; Saito, M.; Nakano, M. *Chem. - Eur. J.* **2016**, *22*, 1493−1500. (f) Zeng, Z.; Shi, X.; Chi, C.; Navarrete, J. T. L.; Casado, J.; Wu, J. *Chem. Soc. Rev.* **2015**, *44*, 6578−6596. (g) Kamada, K.; Ohta, K.; Kubo, T.; Shimizu, A.; Morita, Y.; Nakasuji, K.; Kishi, R.; Ohta, S.; Furukawa, S.-I.; Takahashi, H.; Nakano, M. *Angew. Chem., Int. Ed.* **2007**, *46*, 3544−3546. (h) Kamada, K.; Fuku-en, S.-I.; Minamide, S.; Ohta, K.; Kishi, R.; Nakano, M.; Matsuzaki, H.; Okamoto, H.; Higashikawa, H.; Inoue, K.; Kojima, S.; Yamamoto, Y. *J. Am. Chem. Soc.* **2013**, *135*, 232−241. (i) Nakano, M.; Champagne, B. *J. Phys. Chem. Lett.* **2015**, *6*, 3236−3256. (j) Zeng, Z.; Lee, S.; Son, M.; Fukuda, K.; Burrezo, P. M.; Zhu, X.; Qi, Q.; Li, R.-W.; Navarrete, J. T. L.; Ding, J.; Casado, J.; Nakano, M.; Kim, D.; Wu, J. *J. Am. Chem. Soc.* **2015**, *137*, 8572−8583.
(38) (a) Becke, A. D. *J. Chem. Phys.* **1993**, *98*, 5648−5652. (a1) Stephens, P. J.; Devlin, F. J.; Chabalowski, C. F.; Frisch, M. J. *J. Phys. Chem.* **1994**, *98*, 11623−11627. (b) Frish, M. J.; Trucks, G. W.; Schlegel, H. B.; Scuseria, G. E.; Robb, M. A.; Cheeseman, J. R.; Scalmani, G.; Barone, V.; Mennucci, B.; Petersson, G. A.; Nakatsuji, H.; Caricato, M.; Li, X.; Hratchian, H. P.; Izmaylov, A. F.; Bloino, J.; Zheng, G.; Sonnenberg, J. L.; Hada, M.; Ehara, M.; Toyota, K.; Fukuda, R.; Hasegawa, J.; Ishida, M.; Nakajima, T.; Honda, Y.; Kitao, O.; Nakai, H.; Vreven, T.; Montgomery, J. A., Jr.; Peralta, J. E.; Ogliaro, F.; Bearpark, M.; Heyd, J. J.; Brothers, E.; Kudin, K. N.; Staroverov, V. N.; Keith, T.; Kobayashi, R.; Normand, J.; Raghavachari, K.; Rendell, A.; Burant, J. C.; Iyengar, S. S.; Tomasi, J.; Cossi, M.; Rega, N.; Millam, J. M.; Klene, M.; Knox, J. E.; Cross, J. B.; Bakken, V.; Adamo, C.; Jaramillo, J.; Gomperts, R.; Stratmann, R. E.; Yazyev, O.; Austin, A. J.; Cammi, R.; Pomelli, C.; Ochterski, J. W.; Martin, R. L.; Morokuma, K.; Zakrzewski, V. G.; Voth, G. A.; Salvador, P.; Dannenberg, J. J.; Dapprich, S.; Daniels, A. D.; Farkas, O.; Foresman, J. B.; Ortiz, J. V.; Cioslowski, J.; Fox, D. J. *Gaussian 09*, revision D.01; Gaussian, Inc.: Wallingford, CT, 2013.
(39) Dunning, T. H.; Hay, P. J. In *Modern Theoretical Chemistry*; Schaefer, H. F., III, Ed.; Plenum Press: New York, 1977, Vol. 3, pp 1−28.
(40) (a) Song, L.; Mo, Y.; Zhang, Q.; Wu, W. J. *J. Comput. Chem.* **2005**, *26*, 514−521. (b) Chen, Z.; Ying, F.; Chen, X.; Song, J.; Su, P.; Song, L.; Mo, Y.; Zhang, Q.; Wu, W. *Int. J. Quantum Chem.* **2015**, *115*, 731−737.
(41) (a) Hehre, W. J.; Stewart, R. F.; Pople, J. A. *J. Chem. Phys.* **1969**, *51*, 2657−2664. (b) Dunning, T. H., Jr *J. Chem. Phys.* **1989**, *90*, 1007−1023.
(42) Hirao, K.; Nakano, H.; Nakayama, K.; Dupuis, M. *J. Chem. Phys.* **1996**, *105*, 9227−9239.
(43) Mo, Y.; Lin, Z.; Wu, W.; Zhang, Q. *J. Phys. Chem.* **1996**, *100*, 11569−11572.
(44) Coulson, C. A. *Proc. R. Soc. London, Ser. A* **1939**, *169*, 413.
(45) (a) Goddard, W. A., III; Dunning, T. H.; Hunt, W. J.; Hay, P. J. *Acc. Chem. Res.* **1973**, *6*, 368−376. (b) Goodgame, M. M.; Goddard, W. A., III *Phys. Rev. Lett.* **1985**, *54*, 661−664.
(46) Cooper, D. L.; Gerratt, J.; Raimondi, M. *Chem. Rev.* **1991**, *91*, 929−964.
(47) Coulson, C. A.; Fischer, I. *Philos. Mag.* **1949**, *40*, 386−393.
(48) (a) Bobrowicz, F. W.; Goddard, W. A., III In *Methods of Electronic Structure Theory*; Schaefer, H. F., III, Ed.; Plenum: New York, 1990. (b) Cooper, D. L.; Gerratt, J.; Raimondi, M. *Chem. Rev.* **1991**, *91*, 929−964.
(49) Libit, L.; Hoffmann, R. *J. Am. Chem. Soc.* **1974**, *96*, 1370−1383.
(50) Helliwell, M.; Liaaen-Jensen, S.; Wilkinson, J. *Acta Crystallogr., Sect. C: Cryst. Struct. Commun.* **2008**, *64*, o252.
(51) Kaupp, M.; Danovich, D.; Shaik, S. *Coord. Chem. Rev.* **2017**, *344*, 355−362.
(52) Daudey, J. P.; Trinquier, G.; Barthelat, J. C.; Malrieu, J. P. *Tetrahedron* **1980**, *36*, 3399−3401.
(53) (a) Jia, J.; Wu, H.; Chen, Z.; Mo, Y. *Eur. J. Org. Chem.* **2013**, *2013*, 611−616. (b) Wu, J. I.; Fernandez, I.; Mo, Y.; Schleyer, P. v. R. *J. Chem. Theory Comput.* **2012**, *8*, 1280−1287. (c) Wu, J. I.-C.; Schleyer, P. v. R. *Pure Appl. Chem.* **2013**, *85*, 921−940. (d) Mo, Y.; Gao, J. *Acc. Chem. Res.* **2007**, *40*, 113−119.
(54) Hiberty, P. C. *Isr. J. Chem.* **1983**, *23*, 10−20.
(55) (a) Paci, I.; Johnson, J. C.; Chen, X. D.; Rana, G.; Popović, D.; David, D. E.; Nozik, A. J.; Ratner, M. A.; Michl, J. *J. Am. Chem. Soc.* **2006**, *128*, 16546−16553. (b) Minami, T.; Ito, S.; Nakano, M. *J. Phys. Chem. Lett.* **2012**, *3*, 2719−2723. (c) Ito, S.; Minami, T.; Nakano, M. *J. Phys. Chem. C* **2012**, *116*, 19729−19736. (d) Minami, T.; Nakano, M. *J. Phys. Chem. Lett.* **2012**, *3*, 145−150. (e) Minami, T.; Ito, S.; Nakano, M. *J. Phys. Chem. Lett.* **2013**, *4*, 2133−2137.
(56) Hu, P.; Lee, S.; Herng, T. S.; Aratani, N.; Gonçalves, T. P.; Qi, Q.; Shi, X.; Yamada, H.; Huang, K.-W.; Ding, J.; Kim, D.; Wu, J. *J. Am. Chem. Soc.* **2016**, *138*, 1065−1077.
(57) Braida, B.; Walter, C.; Engels, B.; Hiberty, P. C. *J. Am. Chem. Soc.* **2010**, *132*, 7631−7637.
(58) Stuyver, T.; Fias, S.; De Proft, F.; Geerlings, P.; Tsuji, Y.; Hoffmann, R. *J. Chem. Phys.* **2017**, *146*, 092310.
(59) (a) Angliker, H.; Rommel, E.; Wirz, J. *Chem. Phys. Lett.* **1982**, *87*, 208−212. (b) Houk, K. N.; Lee, P. S.; Nendel, M. *J. Org. Chem.* **2001**, *66*, 5517−5521.
(60) (a) Bachler, V.; Olbrich, G.; Neese, F.; Wieghardt, K. *Inorg. Chem.* **2002**, *41*, 4179. (b) Hayes, E. F.; Siu, A. K. Q. *J. Am. Chem. Soc.* **1971**, *93*, 2090. (c) Kamada, K.; Ohta, K.; Shimizu, A.; Kubo, T.; Kishi, R.; Takahashi, H.; Botek, E.; Champagne, B.; Nakano, M. *J. Phys. Chem. Lett.* **2010**, *1*, 937. (d) Bonacic- Koutecký, V.; Koutecký,

DOI: 10.1021/jacs.7b04410
J. Am. Chem. Soc. 2017, 139, 9302−9316

J.; Michl, J. *Angew. Chem., Int. Ed. Engl.* **1987**, *26*, 170. (e) Nakano, M. *Chem. Rec.* **2017**, *17*, 27−62. (f) Yamaguchi, K. *Chem. Phys. Lett.* **1975**, *33*, 330. (g) Staroverov, V. N.; Davidson, E. R. *Chem. Phys. Lett.* **2000**, *330*, 161. (g1) Head-Gordon, M. *Chem. Phys. Lett.* **2003**, *372*, 508. (h) Yamaguchi, K. Instability in Chemical Bonds. SCF, APUMP, APUCC, MR-CI and MR-CC approaches. In *Self-Consistent Field: Theory and Applications*; Carbo, R., Klobukowski, M., Eds.; Elsevier, Amsterdam, 1990; pp 727−823.

(61) Shaik, S.; Shurki, A. *Angew. Chem., Int. Ed.* **1999**, *38*, 586−625.

(62) Usharani, D.; Lai, W.; Li, C.; Chen, H.; Danovich, D.; Shaik, S. *Chem. Soc. Rev.* **2014**, *43*, 4968−4988.

(63) The equation for the barrier is $\Delta E^* = f G - B$. Here G is the sum of the triplet excitations which is 31 and 22.2 kcal mol^{-1} (for $C_{20}H_{22}$ and $C_{28}H_{30}$) f = 0.3, and B is the resonance energy of the *TS*, which is at least 20 kcal/mol for such a case. Hence, the barrier is very low. Even for 1,4-QDM where G = 82 kcal mol^{-1}, the equation predicts a barrier close to zero.

(64) Shaik, S.; Hiberty, P. C. *J. Am. Chem. Soc.* **1985**, *107*, 3089−3095.

DOI: 10.1021/jacs.7b04410
J. Am. Chem. Soc. 2017, 139, 9302−9316